

ADVANCE INFORMATION COPY
FOR RETENTION OR RETURN TO CODE 2628

4000
NRL Report 7775

7700

Filter and Film Method of Measuring the Temperature of a Hot, Dense, Low-Z Plasma from its Quantum Bremsstrahlung

KENT A. GERBER AND B. GRANT LOGAN

*Plasma Applications Branch
Plasma Physics Division*

July 23, 1974



NAVAL RESEARCH LABORATORY
Washington, D.C.

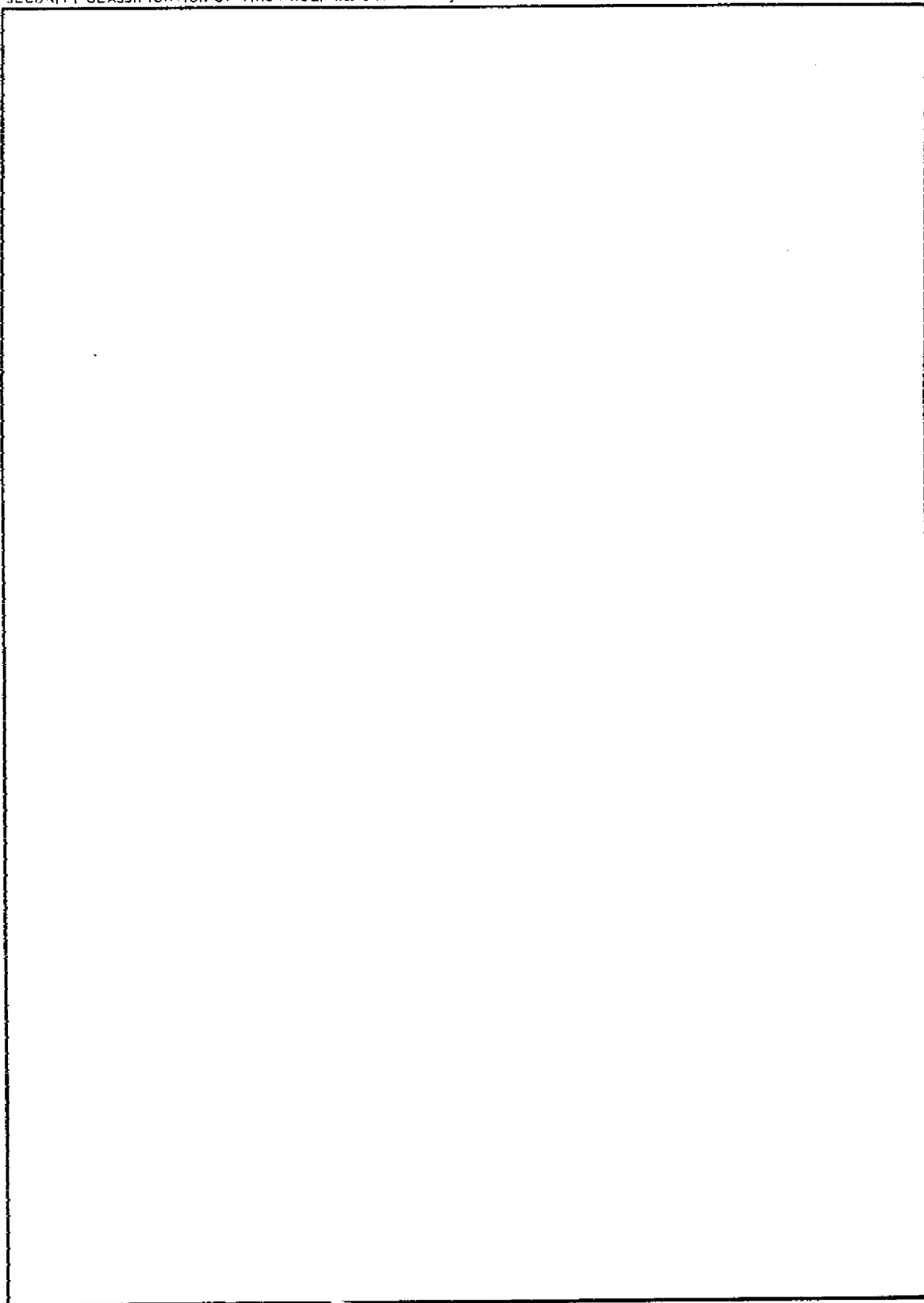
Approved for public release; distribution unlimited.

REPORT DOCUMENTATION PAGE		READ INSTRUCTIONS BEFORE COMPLETING FORM
1. REPORT NUMBER NRL Report 7775	2. GOVT ACCESSION NO.	3. RECIPIENT'S CATALOG NUMBER
4. TITLE (and Subtitle) FILTER AND FILM METHOD OF MEASURING THE TEMPERATURE OF A HOT, DENSE, LOW-Z PLASMA FROM ITS QUANTUM BREMSSTRAHLUNG	5. TYPE OF REPORT & PERIOD COVERED A final report on one phase of a continuing NRL problem.	
	6. PERFORMING ORG. REPORT NUMBER	
7. AUTHOR(s) Kent A. Gerber and B. Grant Logan	8. CONTRACT OR GRANT NUMBER(s)	
9. PERFORMING ORGANIZATION NAME AND ADDRESS Naval Research Laboratory Washington, D.C. 20375	10. PROGRAM ELEMENT, PROJECT, TASK AREA & WORK UNIT NUMBERS NRL Problem H02-28B RR011-09-41/4912	
11. CONTROLLING OFFICE NAME AND ADDRESS Department of the Navy Office of Naval Research Arlington, VA. 22217	12. REPORT DATE July 23, 1974	
	13. NUMBER OF PAGES 23	
14. MONITORING AGENCY NAME & ADDRESS (if different from Controlling Office)	15. SECURITY CLASS. (of this report) Unclassified	
	15a. DECLASSIFICATION/DOWNGRADING SCHEDULE	
16. DISTRIBUTION STATEMENT (of this Report) Approved for public release; distribution unlimited.		
17. DISTRIBUTION STATEMENT (of the abstract entered in Block 20, if different from Report)		
18. SUPPLEMENTARY NOTES		
19. KEY WORDS (Continue on reverse side if necessary and identify by block number) Plasmas X-ray bremsstrahlung Electron temperature X-ray transmission curves Thin metallic foils X-ray film detector		
20. ABSTRACT (Continue on reverse side if necessary and identify by block number) Results of calculations of the total integrated x-ray quantum bremsstrahlung emission transmitted through absorbers of aluminum, copper and carbon (polyethylene) are presented for a range of plasma temperatures and absorber thickness for both ideal detectors and for film. Such information is useful in obtaining values for the electron temperature in a plasma from measurements of the x-ray continuum emission.		

DD FORM 1473
1 JAN 73EDITION OF 1 NOV 65 IS OBSOLETE
S/N 0102-014-6601

i

SECURITY CLASSIFICATION OF THIS PAGE (When Data Entered)



CONTENTS

INTRODUCTION	1
COMPUTATION	1
Considerations of the Spectral Power Density	1
Numerical Considerations	2
Calculations	2
RESULTS AND DISCUSSION	3
INTERPRETATION	4
CONCLUSION	4
REFERENCES	4

**FILTER AND FILM METHOD OF MEASURING
THE TEMPERATURE OF A HOT, DENSE, LOW-Z PLASMA
FROM ITS QUANTUM BREMSSTRAHLUNG**

INTRODUCTION

The filter method, used to measure temperatures of a low-Z (hydrogen or helium), Maxwellian plasma through its bremsstrahlung emission, has been widely used since it was first applied by Jahoda and coworkers to the Scylla θ -pinch [1, 2]. The method conveniently diagnoses the electron temperature beyond the normal range of other commonly used diagnostic methods such as Thomson scattering of laser light [3]. The first attempts at systematization of the method was done by Elton and Anderson [4], later extended by Elton [5]; other works exist by Peacock [6], Adams and Taylor [7], and Bogan [8], to cite a few. References 4 through 8 assume a classical bremsstrahlung. In an effort to include the quantum-mechanical alterations to the classical bremsstrahlung spectra, Robouch and Rager [9] have used the free-free transition Gaunt factors [10] in their calculations, as well as to account for the energy-dependent efficiency of real detectors, namely silicon solid-state diodes. The present work uses an adequate quantum-mechanical theory for the bremsstrahlung spectrum, so that Gaunt factors are not needed, and presents graphs of the bremsstrahlung emission transmitted through various thicknesses of a number of absorbers and detected by Kodak No-Screen Medical X-ray film*.

COMPUTATION

Considerations of the Spectral Power Density

The spectral power density of the bremsstrahlung emission as a function of the photon energy $h\nu$ and the plasma (Maxwellian) temperature kT , including the detector response, is

$$P_s(T, h\nu) d(h\nu) = \frac{n_e n_i \int_{h\nu}^{\infty} dE E^{1/2} e^{-E/kT} \sigma(h\nu, E) v_e(E) \frac{1}{R(h\nu)} d(h\nu)}{\int_0^{\infty} dE E^{1/2} e^{-E/kT}}, \quad (1)$$

Note: Manuscript submitted May 30, 1974.

*Film and developer are available from Eastman Kodak Co., Rochester, NY, 14650.

where $\sigma(h\nu, E)$ is the bremsstrahlung emission cross section, E is the electron energy, $v_e(E)$ is the electron velocity, and n_e and n_i are the plasma electron and ion densities respectively; $R(h\nu)$ is the photon-energy-dependent film efficiency. For low- Z (1 or 2) ions and electron energies less than 100 keV, a detailed evaluation [11] of the relativistically correct quantum-mechanical treatment [12] of the cross section shows that the single-electron spectrum can be approximated to within 10% by the nonrelativistic Born-approximation result [13]:

$$\sigma(h\nu, E) = \frac{Z^2 r_0^2}{137} \frac{16}{3} \frac{1}{P_i^2} \ln \left(\frac{P_i + P_f}{P_i - P_f} \right), \quad (2)$$

where

$$P_i = [E(E + 2)]^{1/2},$$

$$P_f = [E_f(E_f + 2)]^{1/2},$$

$$E_f = E - h\nu,$$

and r_0 is the classical electron radius. Use of Eq. (2) in Eq. (1) gives a spectral power density varying more steeply than $e^{-h\nu/kT}$, which one obtains from classical calculations [10].

Numerical Considerations

A computer code was employed to evaluate numerically the integral of the quantum bremsstrahlung since the use of individual integration steps facilitates the inclusion of attenuation-coefficient and film-response data. The integration range in electron energy was taken from two orders of magnitude less to one order of magnitude greater than the temperature kT of the Maxwellian plasma in 150 integration steps. The truncation error in the evaluation of the integral has been shown to be less than 1% over the range of temperatures [11].

Calculation

The present investigation is restricted to a temperature range of 1 to 100 keV. Three absorbers, aluminum, copper, and carbon in the form of polyethylene CH_2 are used as filters. Thicknesses range from 0 to 1 cm. Attenuation coefficients used in the calculation were taken from Allen [14]. The calculated integrated bremsstrahlung emission is normalized to $n_e n_i Z^2$ and has the units of W/cm^3 , power density emitted into 4π steradians.

The film response $R(h\nu)$, in the form of exposure factors, was measured by Dozier et al. [15] for Kodak No-Screen Medical X-ray film over the photon energy range of a few

keV to 1.3 MeV. Except for the Ag and Br edges, the film sensitivity decreases with increasing photon energy. The film factors used in the calculation ranged from 0.1 to 0.002 from 1 to 1000 keV respectively.

RESULTS AND DISCUSSION

Results of the calculation are given in a series of graphs. Figure 1 gives the total emitted power density over the entire temperature range with no absorbers (open), with and without including the film response. The transparency of the film at high energies is evident from the lower curve. One can calculate the absolute power density at any temperature from the open, no-film-factor curve by multiplying its value at the temperature by the factor $n_e n_i Z^2$, where the densities are particles cm^{-3} and Z is either 1 or 2. When the volume of plasma emission and the solid angle of detection are known, one can calculate the power incident on a unit area of the film. The number of incident photons required to give a film neutral-density exposure of 1.00 for example ranges from $1.5 \times 10^7 \text{ cm}^{-2}$ to $2.25 \times 10^8 \text{ cm}^{-2}$ as the photon energy goes from 1 to 100 keV [15].

Figures 2 through 7 are plots of the integrated bremsstrahlung emission transmitted through various thickness of absorbers over the range of electron temperatures. Absolute power densities transmitted through various foils can be calculated from these curves, as previously discussed. Figures 2 through 7, which compare to the curves of Elton [5], can be used in constructing ratios for temperature measurements using detectors whose efficiencies do not depend on photon energy, i.e., ideal detectors. The present results, however, lead to ratios that differ, by an amount detectable experimentally, from those of the classical approach. The differences in ratios for two combinations of aluminum absorbers are shown in Fig. 8. At a ratio of 20, for combination 2 for example, the two calculations yield electron temperatures that differ by about 20%.

The results plotted in Figs. 9 through 14, include the energy-dependent efficiency of the Kodak No-Screen Medical X-ray film. These curves can be related absolutely to the preceding curves without the film response if they are multiplied by 10 to account for the normalization to 0.1 chosen in the calculation. Thus in Fig. 1, for example, the two curves would approach each other at 1 keV, where the film response is nearly unity. These curves have been used in constructing a few yield ratios using various absorber combinations and have been plotted as Fig. 15. The choice of the absorber material and thickness for each "channel" of the detector depends on the temperature range of interest. Selections can be made to give a rapidly changing ratio at any temperature, thus assuring that even a relatively large error in the ratio measurement results in only a small error in the temperature determination.

The range of yield ratios plotted in Fig. 15 goes from 1 to 100. In reality the useful range of ratios is determined by the accuracy of the instrument used to measure the neutral density of the exposed films. If one uses a microdensitometer with a resolution of 0.01 neutral density, the useful range of ratios could be as large as 1 to 200, i.e., $2/2$ to $2/0.01$. The absolute measured neutral density of 2 is taken as an upper limit, since the film no longer responds linearly with exposure beyond this density [15] and this nonlinear response is not considered in the calculation. The standard development procedure for Kodak

No-Screen Medical X-ray film is wet processing for 5 min in fresh Kodak Liquid X-ray Developer at 20° C, rinsing for 30 s in water, fixing in Kodak Liquid X-ray Fixer for 10 min, and washing in running water for 30 min.

INTERPRETATION

Since the film integrates exposure over time, care has to be taken in the interpretation of the measured temperature. If the plasma temperature changes rapidly over the integration time, the measured value will be a weighted average of all the temperatures. However, calculations using specific electron-temperature time-history models show that for the most part the measured temperature will be close to the peak temperature achieved at any time in the time history.

CONCLUSION

The filter and film method of plasma-temperature measurement provides a fast, compact, and inexpensive alternative to other methods such as scintillator-photomultiplier combinations or Si solid-state diodes. The calculations presented here should be applicable to most hot, dense, low-Z Maxwellian plasmas, especially those with Tokamak or other fusion-device parameters.

REFERENCES

1. F.C. Jahoda, E.M. Little, W.E. Quinn, G.A. Sawyer, and T.F. Stratton, *Phys. Rev.* **119**, 843 (1960).
2. T.F. Stratton in *Plasma Diagnostics Techniques*, edited by R.H. Huddlestone and S.L. Leonard, Academic Press, New York, 1965, p. 359.
3. K.A. Gerber, "Laser Scattering System on the NRL Triton Experiment," NRL Memorandum Report 2818, 1974.
4. R.C. Elton and A.D. Anderson, "Calculations Useful in the Determination of Electron Temperature from X-ray Continuum Radiation Emitted from High Temperature Plasmas," NRL Report 6541, 1967.
5. R.C. Elton, "Determination of Electron Temperatures Between 50 eV and 100 keV from X-ray Continuum Radiation in Plasmas," NRL Report 6738, 1968.
6. N. Peacock, Culham Laboratories, Abingdon UK Report CLM-M39, 1964.
7. J.H. Adams and I.C. Taylor, Culham Laboratories, Abingdon UK Report CLM-R81, 1968.
8. P. Bogan in *Plasma Diagnostics*, edited by W. Lochte-Holtgreven, North-Holland, Amsterdam, 1968, p. 424.
9. B.V. Robouch and J.P. Rager, *J. Appl. Phys.* **44**, 1527 (1973).
10. W.J. Karzas and R. Latter, *Astrophys. J. Suppl.* **6**, 167 (1961).

NRL REPORT 7775

11. B.G. Logan, to be published in 1974 as an NRL Memorandum Report.
12. G. Elwert and E. Haug, Phys. Rev. 183, 90 (1969).
13. H.W. Koch and J.W. Motz, Rev. Mod. Phys. 31, 920 (1959).
14. S.J.M. Allen *Handbook of Chemistry and Physics*, 47th Edition, 1966-67, Chemical Rubber Co. Cleveland, 1966, p. E114.
15. C.M. Dozier, J.V. Gilfrich, and L.S. Birks, Appl. Opt. 6, 2136 (1967).

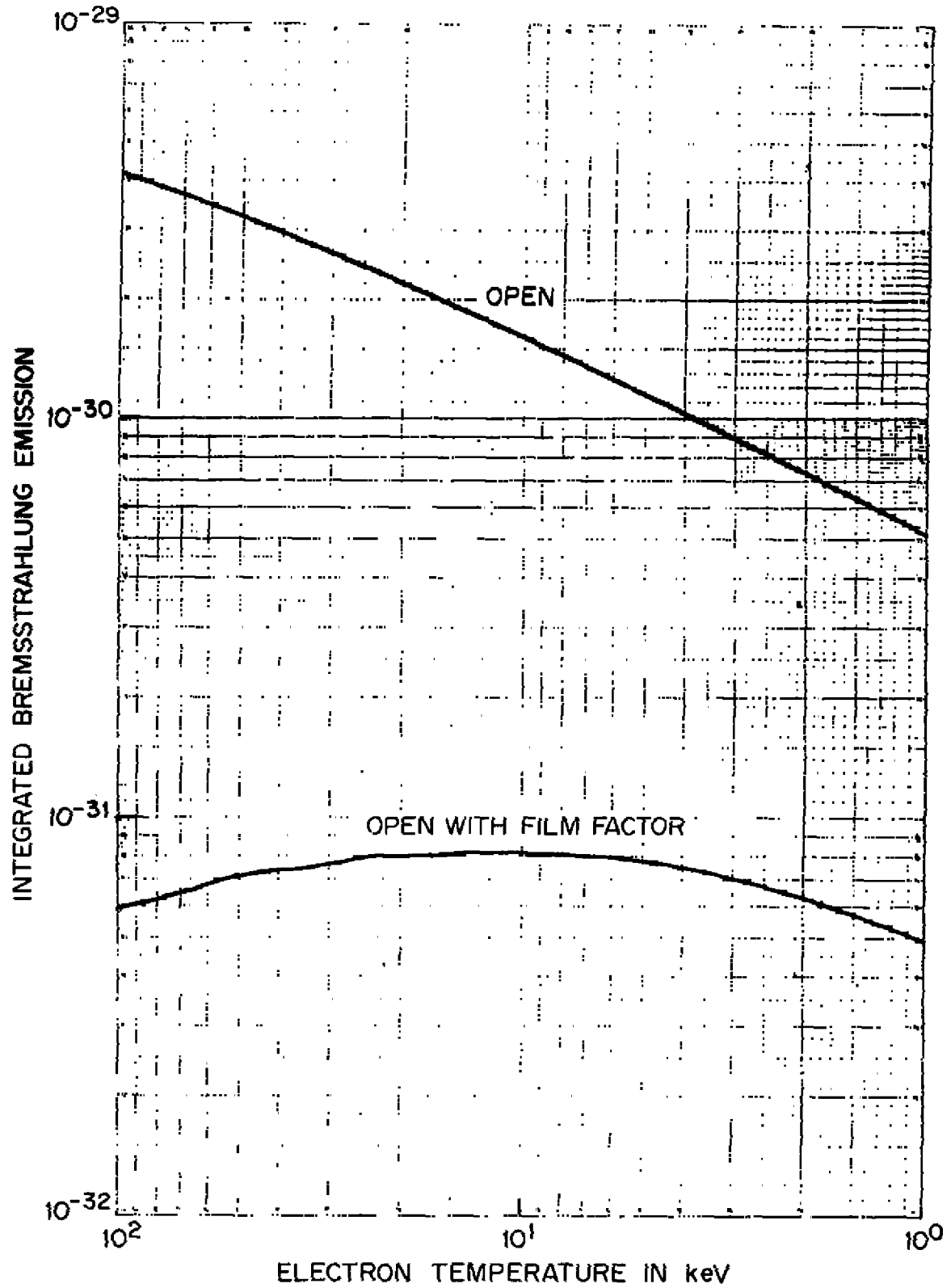


Fig. 1 — Integrated bremsstrahlung emission in W/cm³ vs electron temperature for open "channels", with and without film response

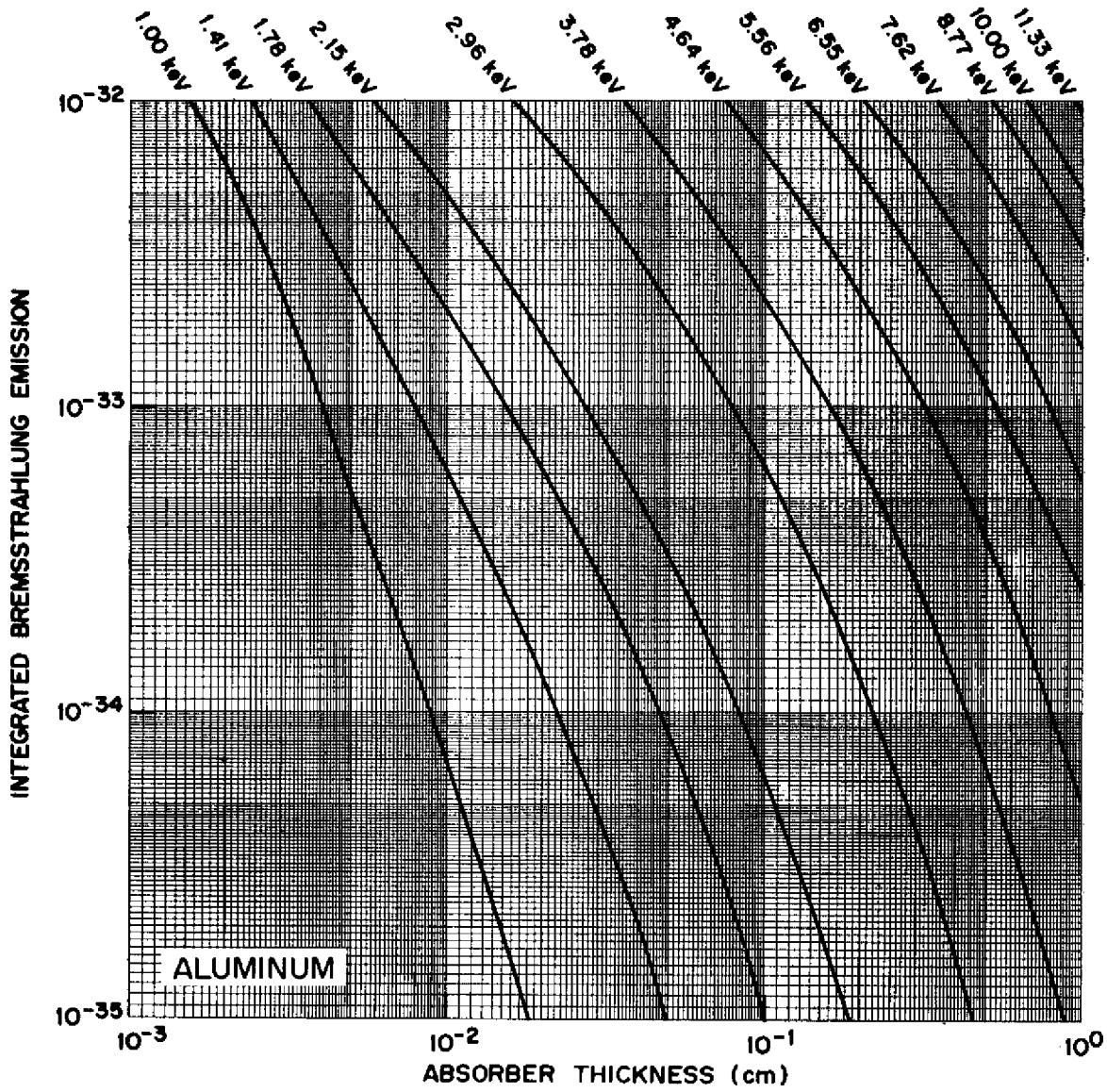


Fig. 2 — Transmitted integrated bremsstrahlung emission in W/cm^3 vs aluminum absorber thickness, without film response, for a range of electron temperatures

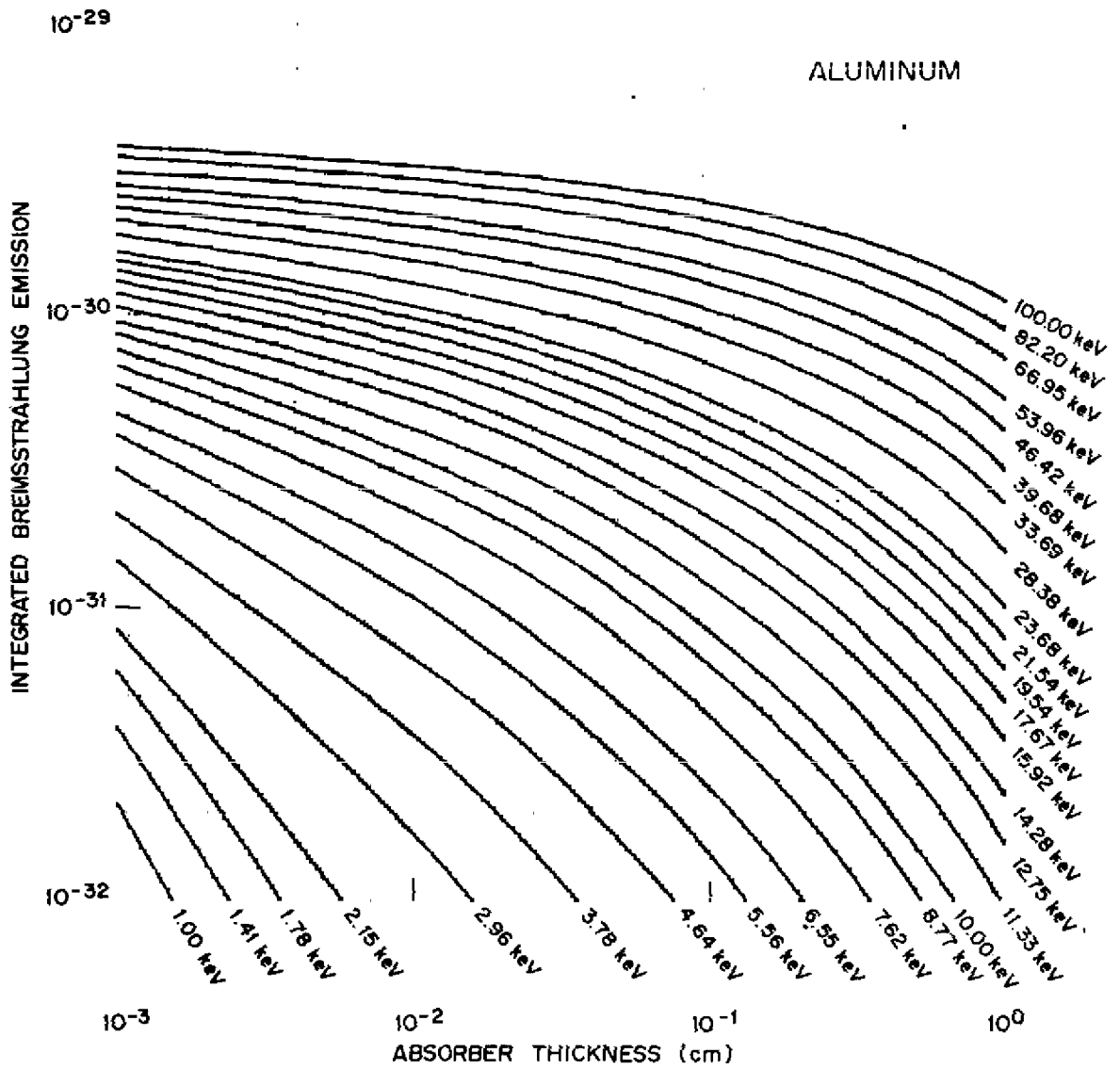


Fig. 3 - Transmitted integrated bremsstrahlung emission in W/cm² vs aluminum absorber thickness, without film response, for a range of electron temperatures

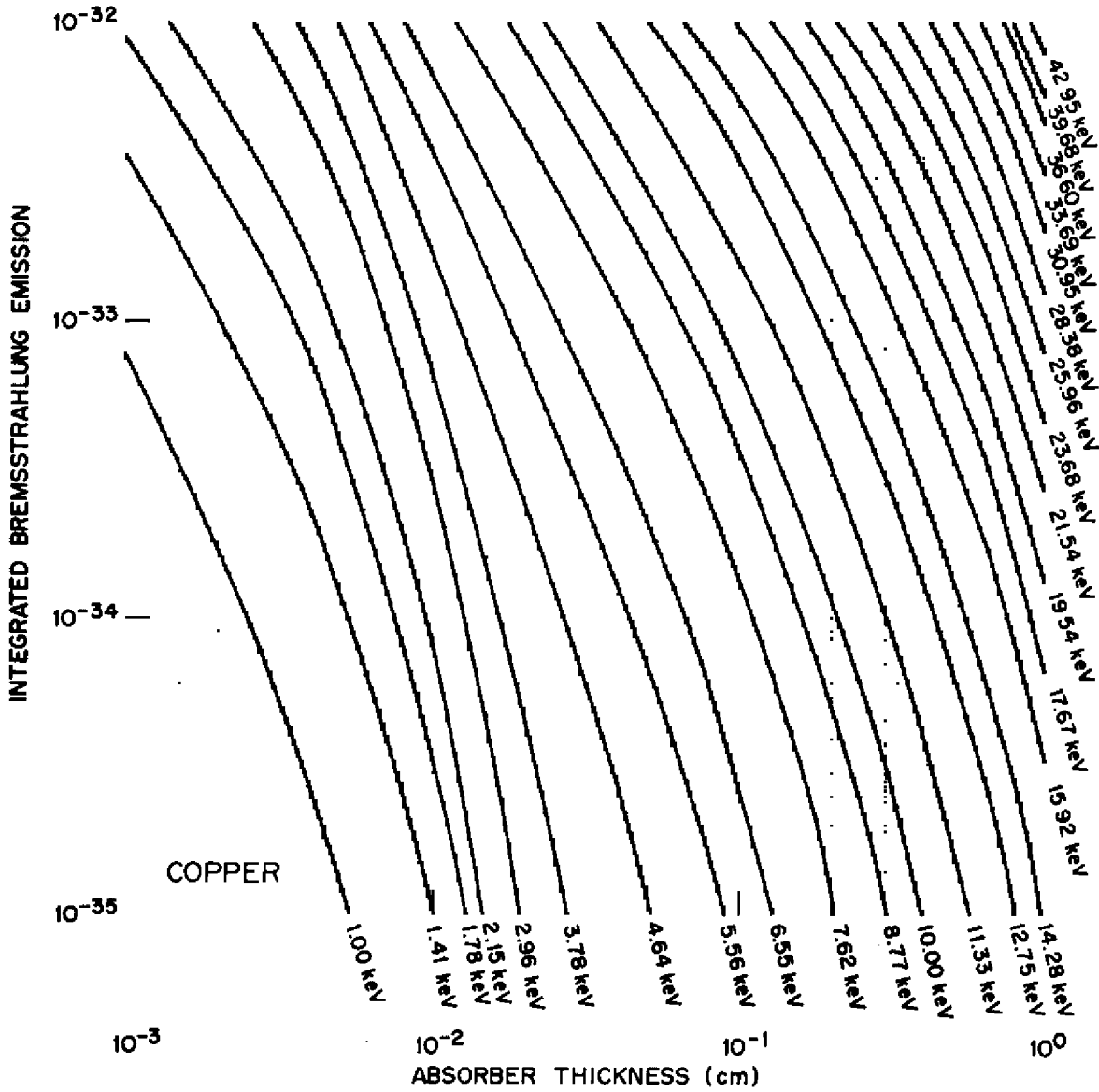


Fig. 4 — Transmitted integrated bremsstrahlung emission in W/cm^3 vs copper absorber thickness, without film response, for a range of electron temperatures

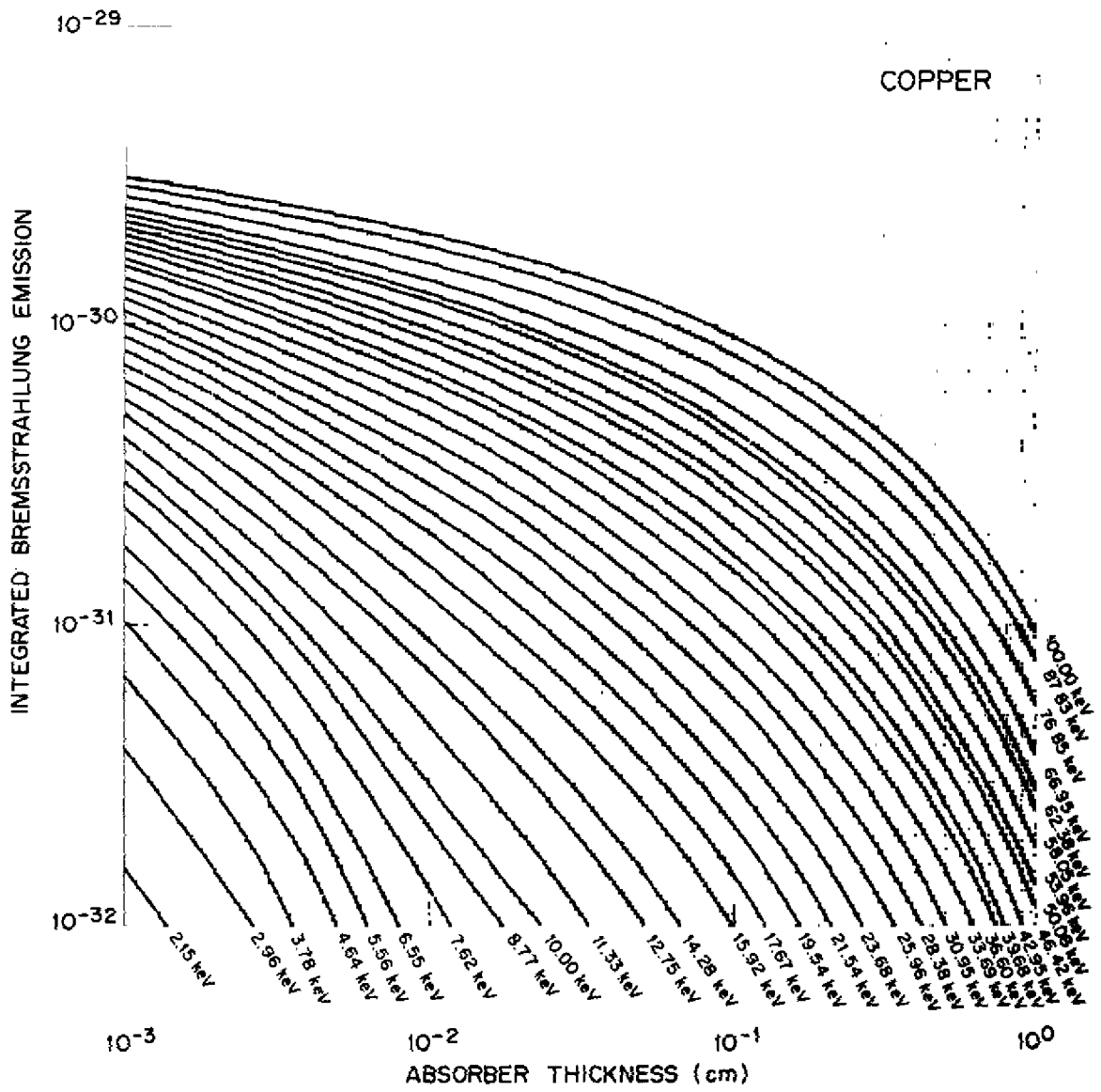


Fig. 5 — Transmitted integrated bremsstrahlung emission in W/cm^3 vs copper absorber thickness, without film response, for a range of electron temperatures

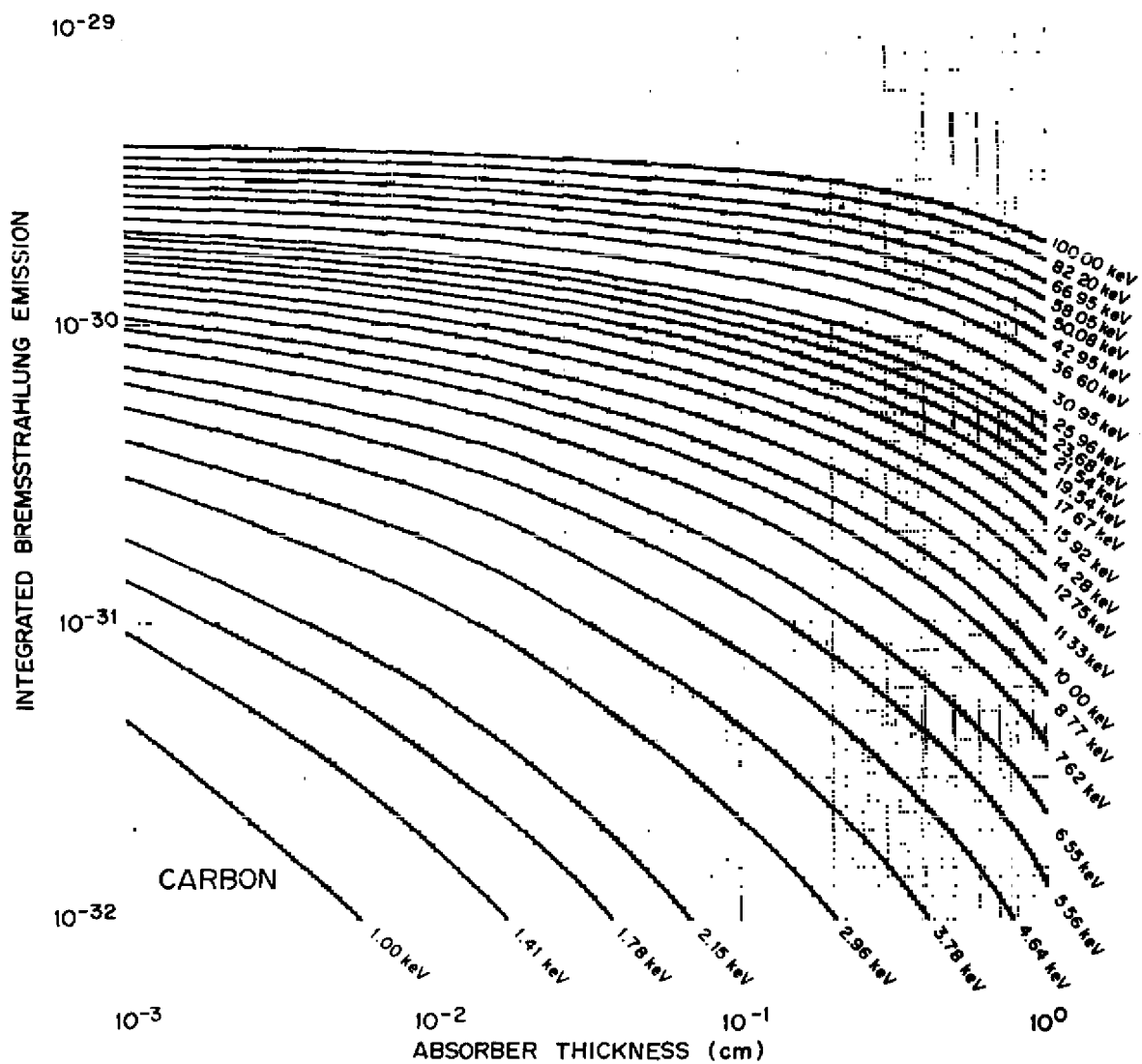


Fig. 6 - Transmitted integrated bremsstrahlung emission in W/cm³ vs carbon (CH₂) absorber thickness without film response for a range of electron temperatures

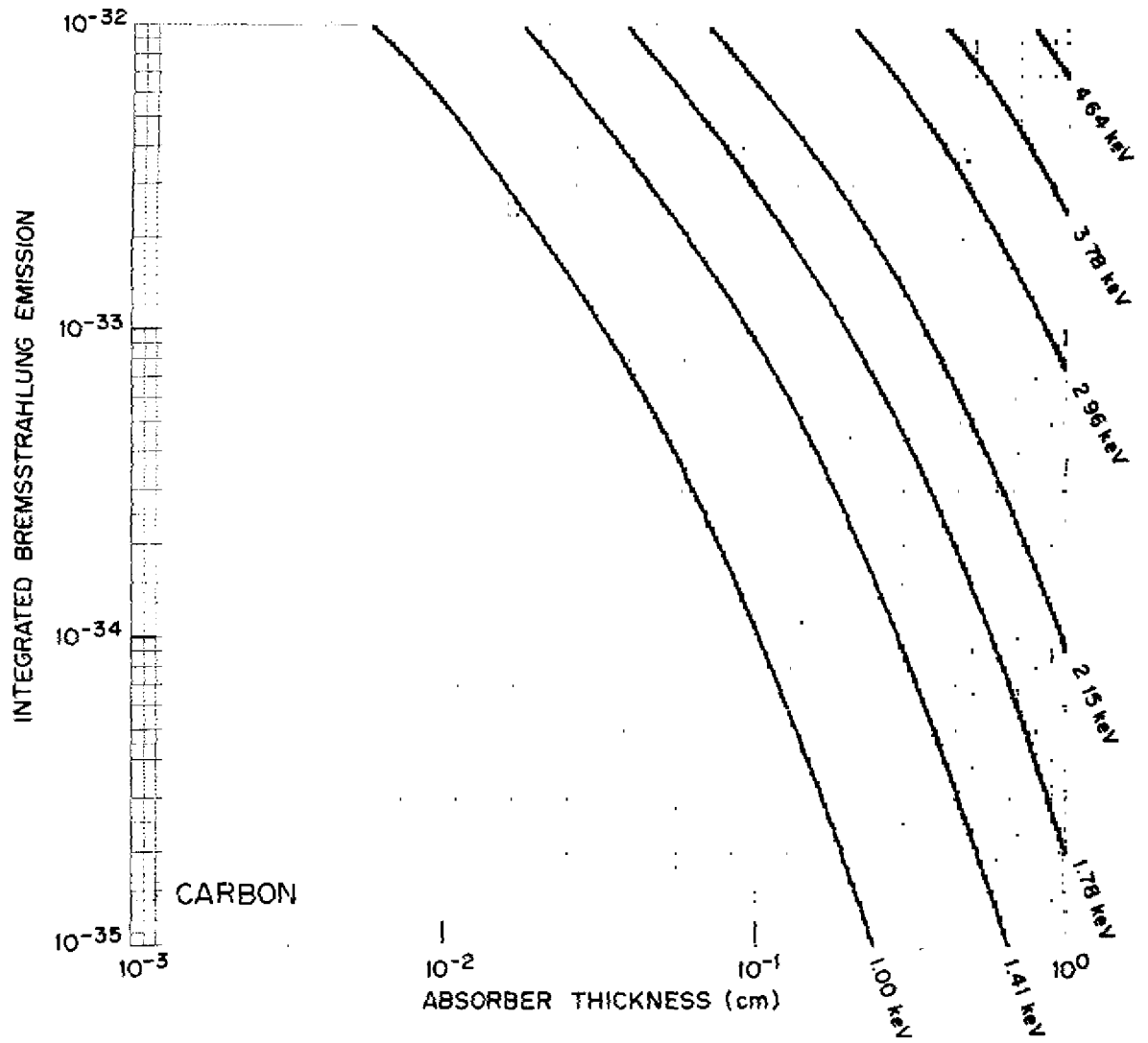


Fig. 7 — Transmitted integrated bremsstrahlung emission in W/cm^3 vs carbon (CH_2) absorber thickness, without film response, for a range of electron temperatures

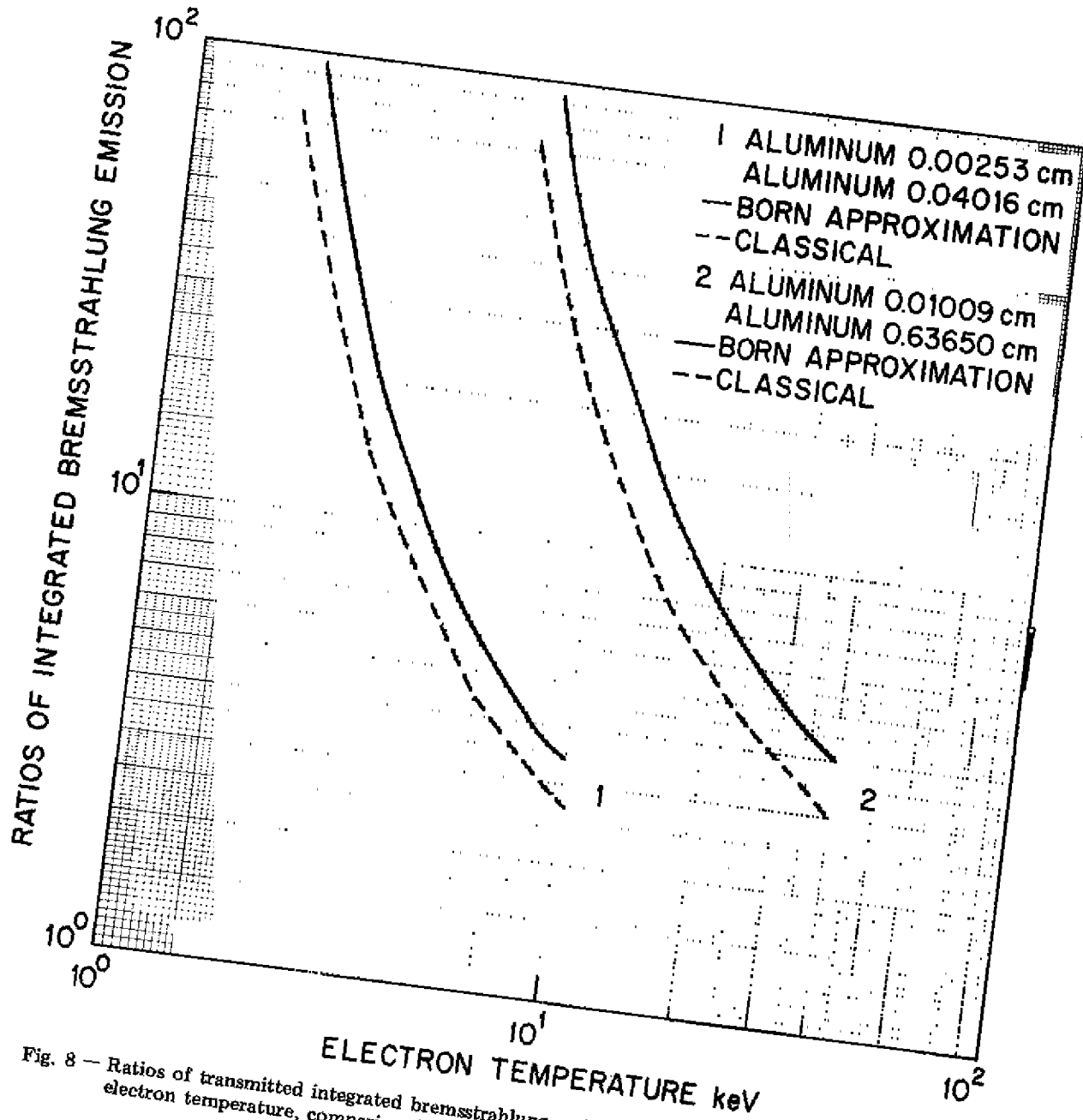


Fig. 8 — Ratios of transmitted integrated bremsstrahlung emission for two absorber combinations vs electron temperature, comparing the Born approximation to classical calculations

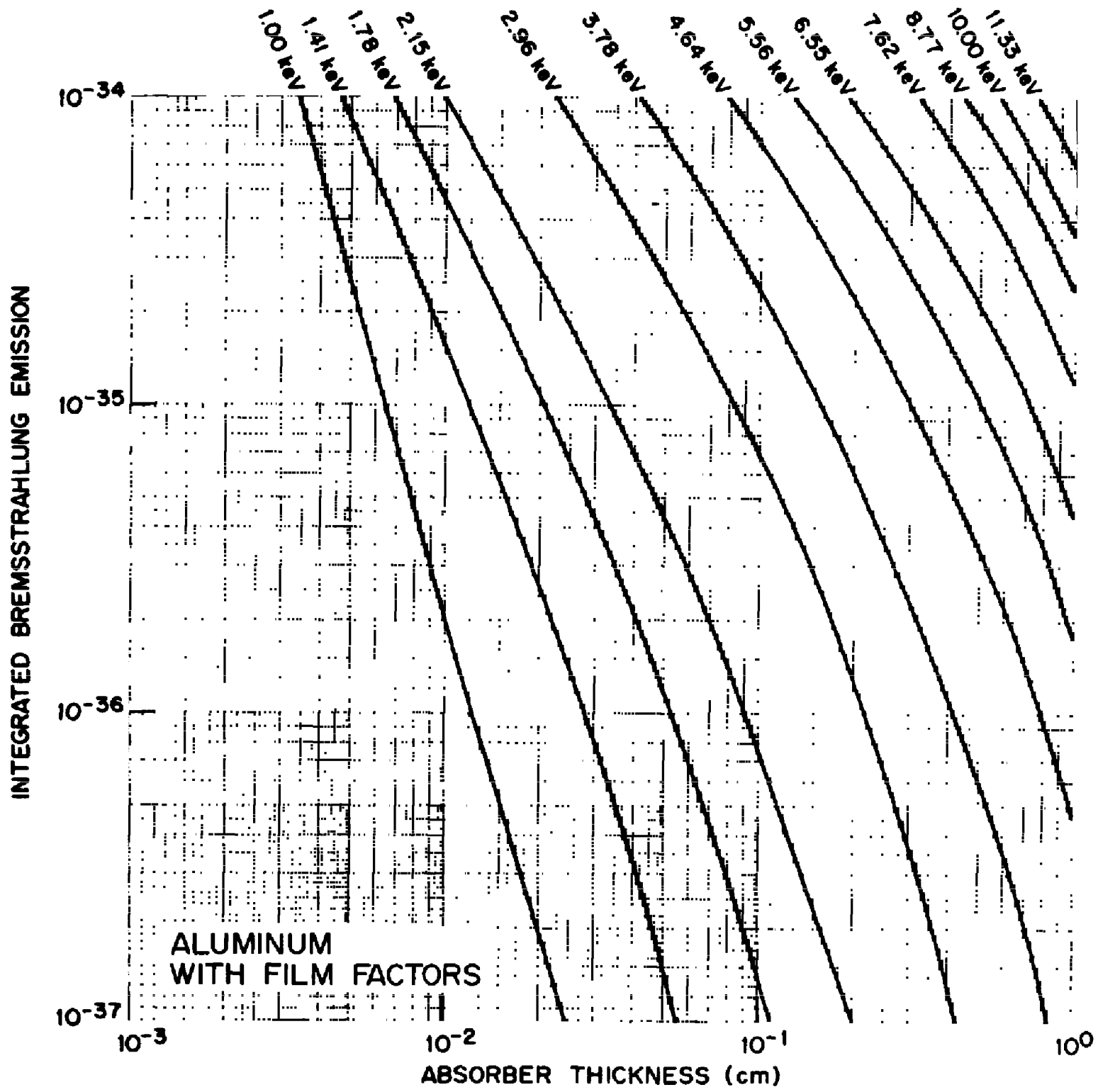


Fig. 9 — Transmitted integrated bremsstrahlung emission in W/cm^3 vs aluminum absorber thickness, including film response, for a range of electron temperatures

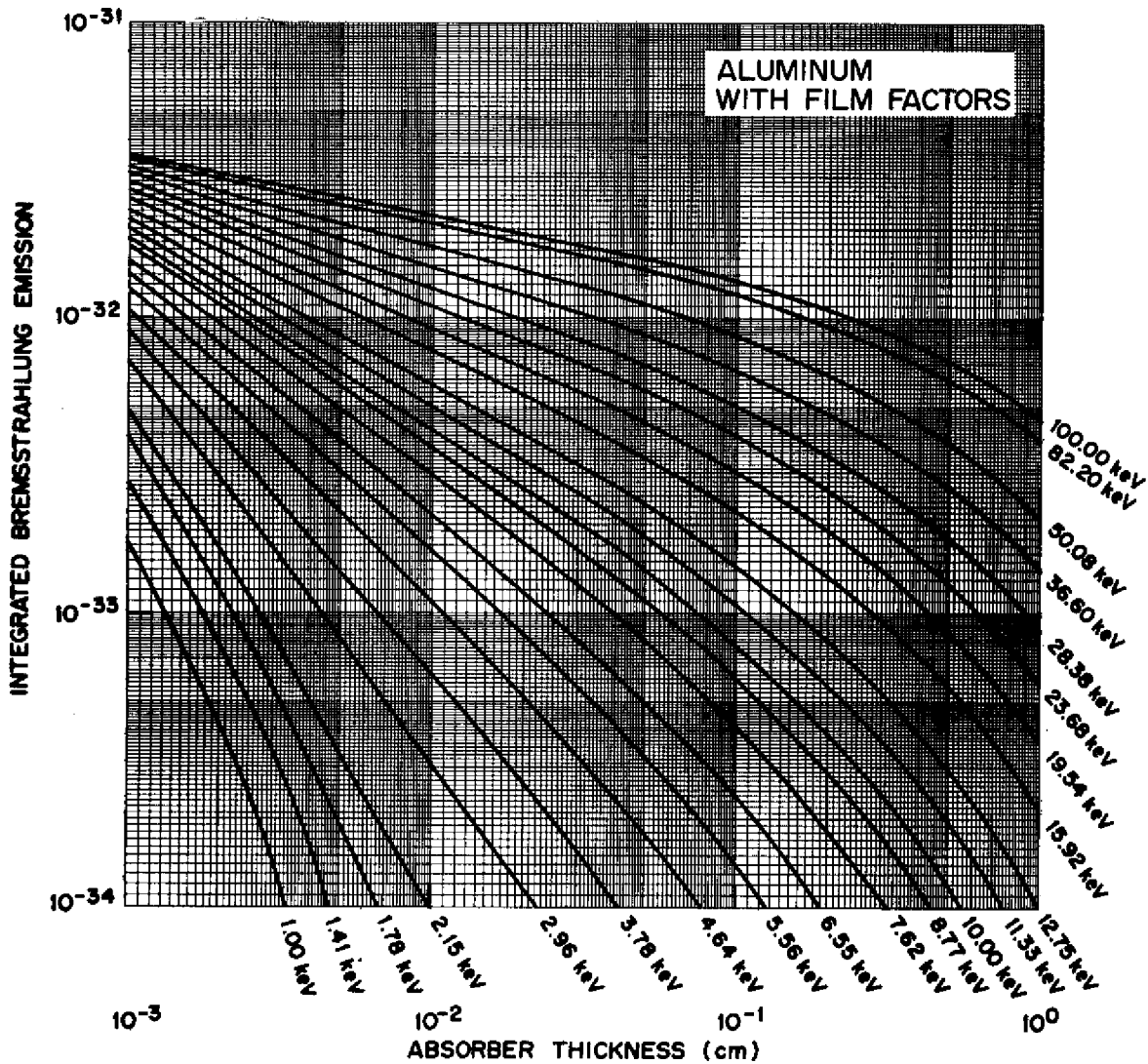


Fig. 10 — Transmitted integrated bremsstrahlung emission in W/cm^3 vs aluminum absorber thickness, including film response, for a range of electron temperatures

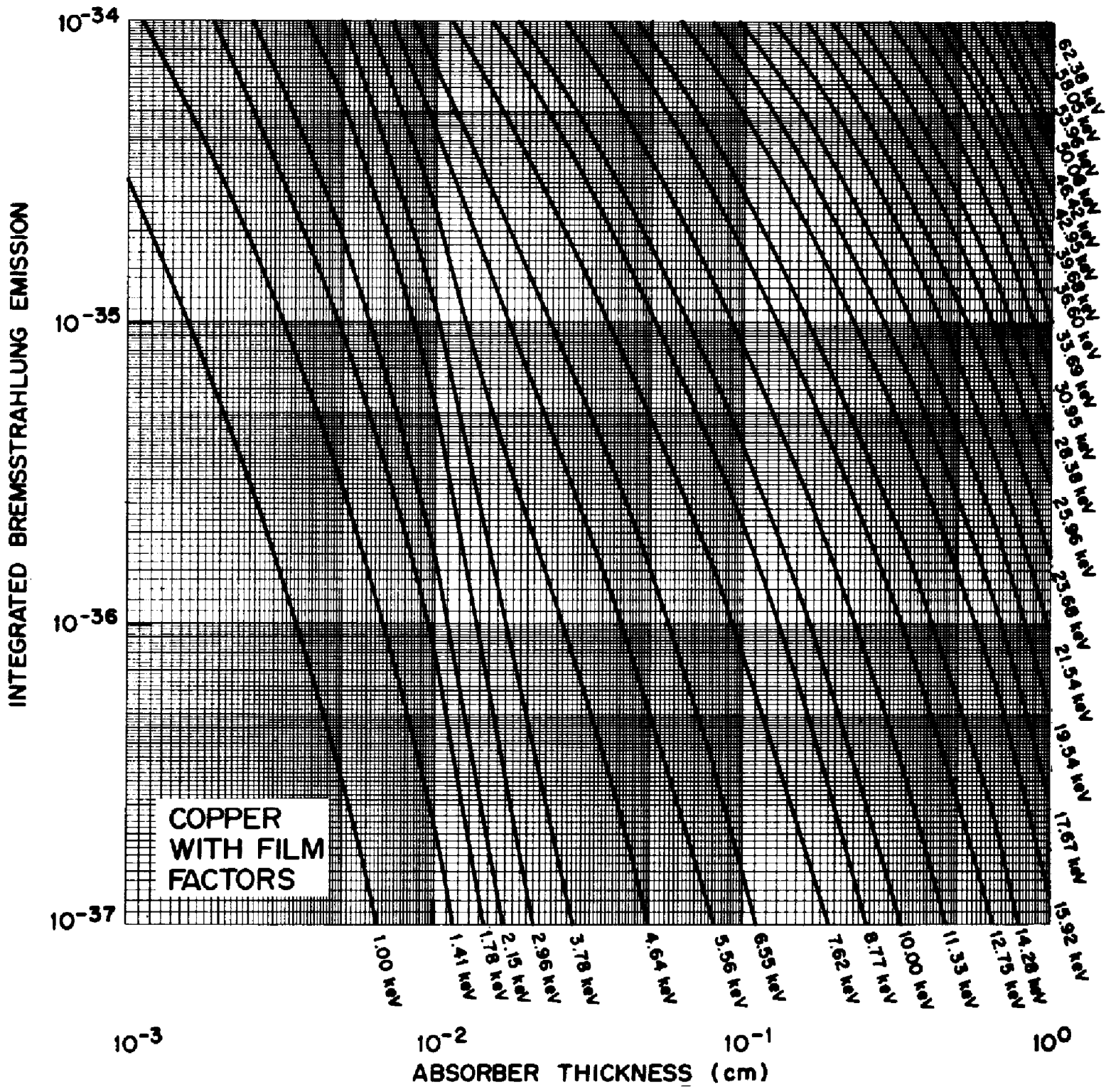


Fig. 11 — Transmitted integrated bremsstrahlung emission in W/cm³ vs copper absorber thickness, including film response, for a range of electron temperatures

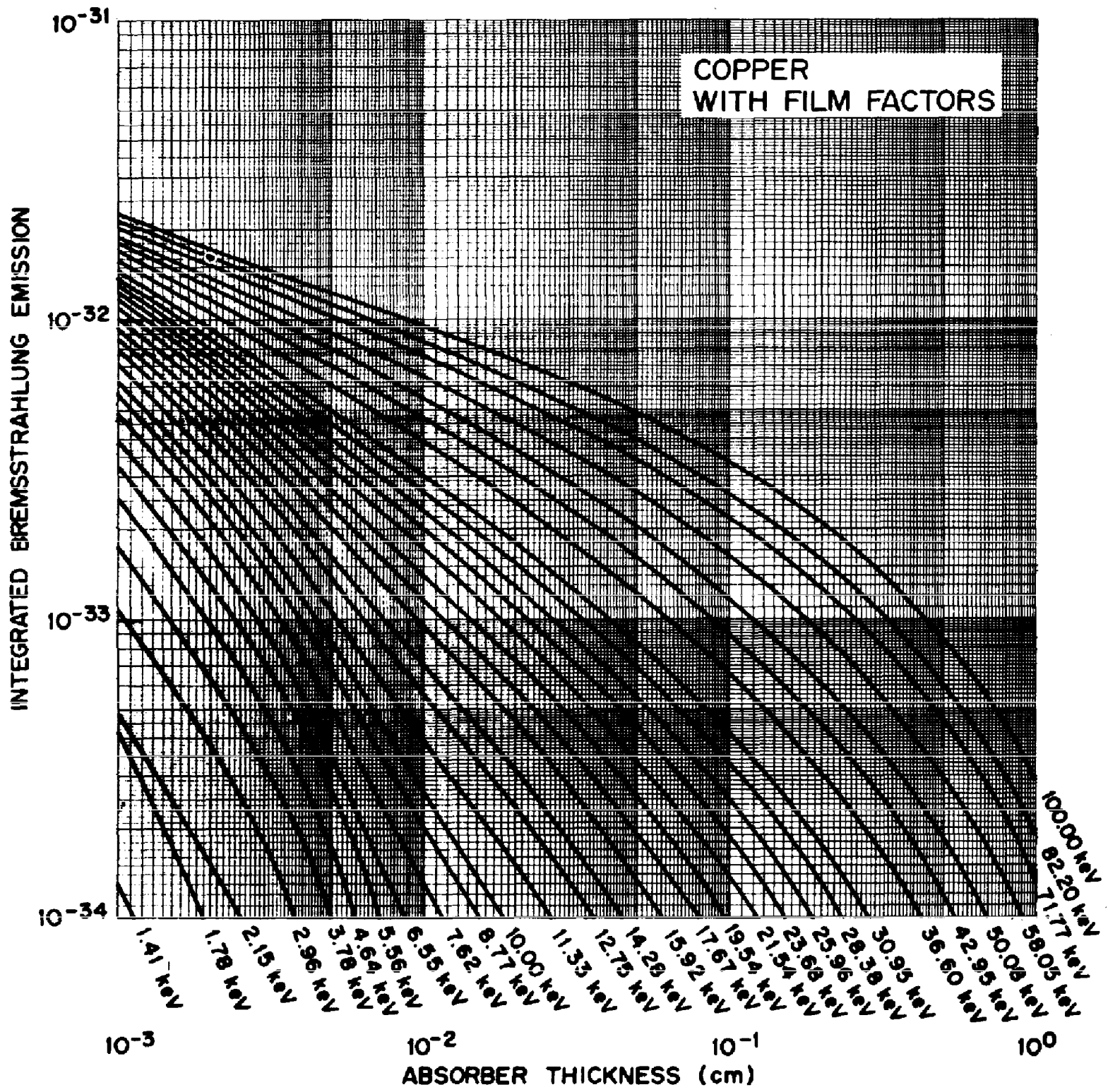


Fig. 12 — Transmitted integrated bremsstrahlung emission in W/cm^3 vs copper absorber thickness, including film response, for a range of electron temperatures

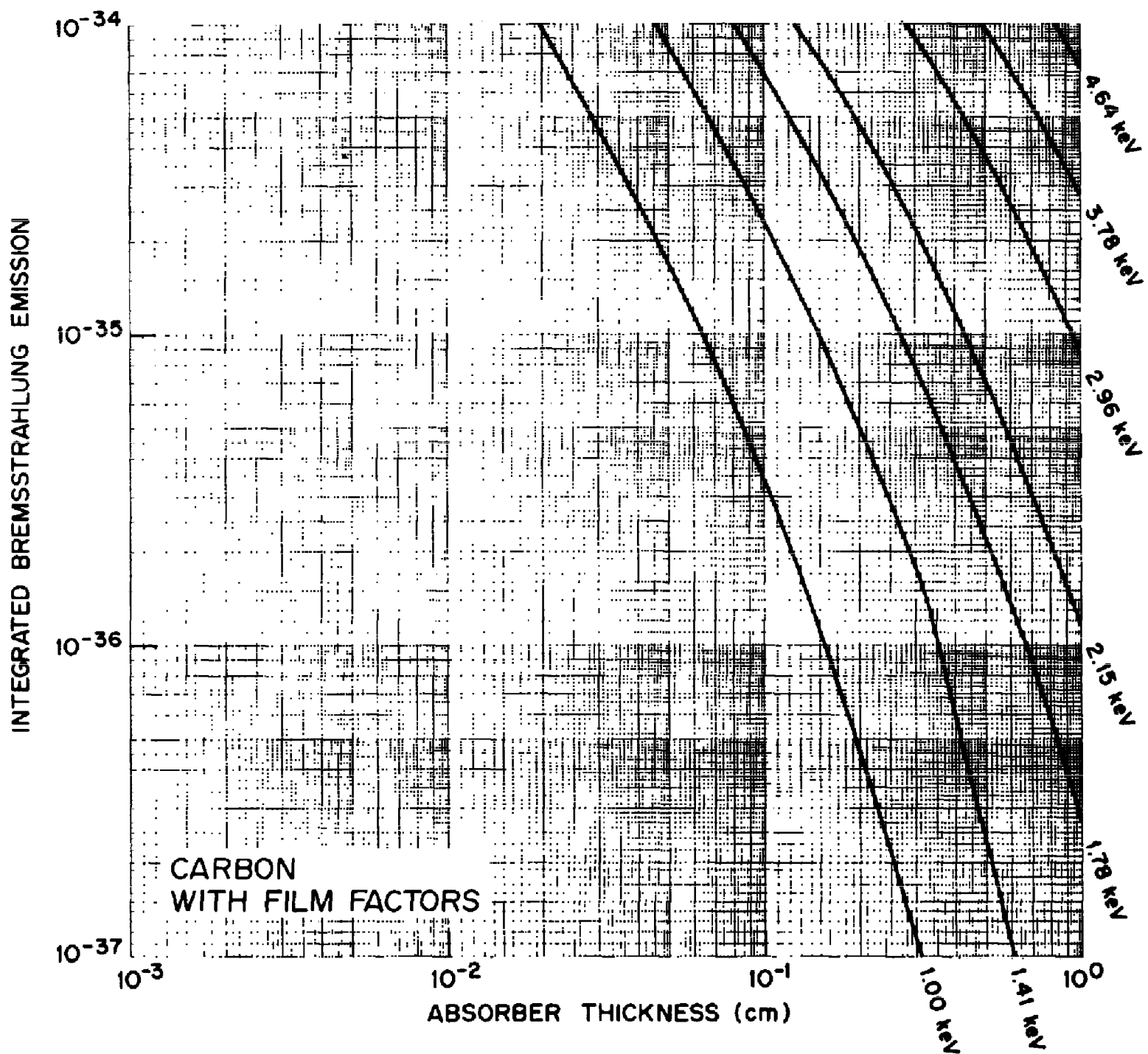


Fig. 13 — Transmitted integrated bremsstrahlung emission in W/cm³ vs carbon (CH₂) absorber thickness, including film response, for a range of electron temperatures

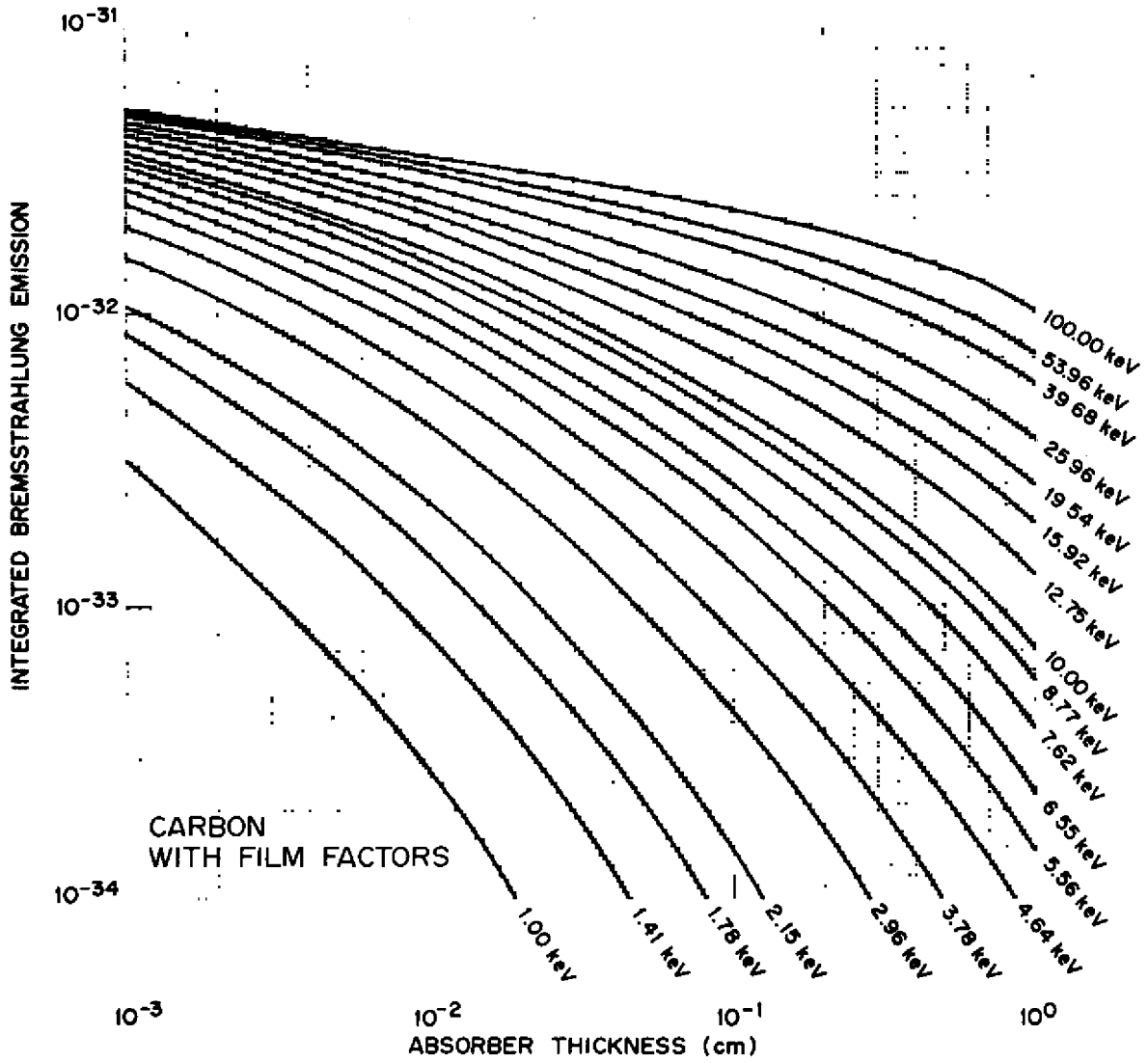


Fig. 14 — Transmitted integrated bremsstrahlung emission in W/cm^3 vs carbon (CH_2) absorber thickness, including film response, for a range of electron temperatures

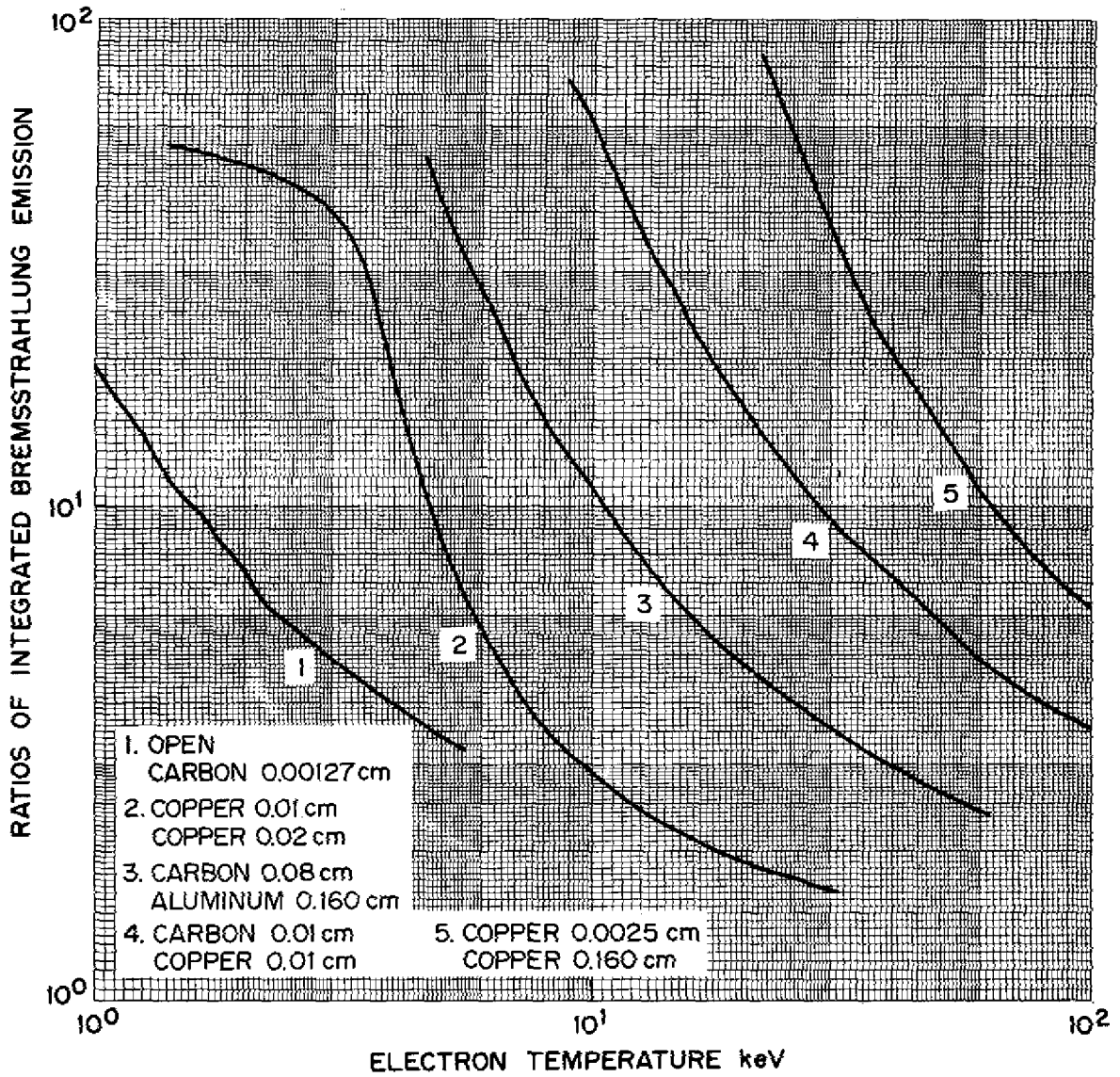


Fig. 15 — Ratios of detected integrated bremsstrahlung emission for five absorber combinations vs electron temperature. These curves were obtained from Figs. 9 through 14.